Iranian Journal of Electrical and Electronic Engineering 01 (2019) 142–150
Special Issue on Power Engineering

IUST Iran University of Science and Technology

Iranian Journal of Electrical and Electronic Engineering

Journal Homepage: ijeee.iust.ac.ir

Sensorless Speed Control of Double Star Induction Machine With Five Level DTC Exploiting Neural Network and Extended Kalman Filter

M. H. Lazreg*(C.A.) and A. Bentaallah*

Abstract: This article presents a sensorless five level DTC control based on neural networks using Extended Kalman Filter (EKF) applied to Double Star Induction Machine (DSIM). The application of the DTC control brings a very interesting solution to the problems of robustness and dynamics. However, this control has some drawbacks such as the uncontrolled of the switching frequency and the strong ripple torque. To improve the performance of the system to be controlled, robust techniques have been applied, namely artificial neural networks. In order to reduce the number of sensors used, and thus the cost of installation, Extended Kalman filter is used to estimate the rotor speed. By viewing the simulation results using the MATLAB language for the control. The results of simulations obtained showed a very satisfactory behaviour of the machine.

Keywords: Double Star Induction Machine, Direct Torque Control (DTC), Five Level Inverter, Artificial Neural Network (ANN), Sensorless Control, Extended Kalman Filter.

1 Introduction

VARIABLE speed electric drives have gained considerable importance in industry and research, and require knowledge in the field of electrical engineering, such as electrical machines, power electronics. Thus, a variable speed drive consists of a power source, a power electronics converter, a machine and a control system.

Multiphase machines offer an interesting alternative to reduce stress on switches and windings. Indeed, the multiplication of the number of phases allows a splitting of the power and thus a reduction of the switched voltages with a given current. In addition, these machines can reduce the amplitude and increase the frequency of torque ripples, allowing the mechanical load to filter more easily. One of the most common examples of multiphase machines is the Double Star Induction Machine (DSIM) [1].

Iranian Journal of Electrical and Electronic Engineering, 2019.
Paper first received 13 June 2018 and accepted 08 September 2018.
* The authors are with the Department of Electrical Engineering, Djillali Liabes University, Sidi Bel Abbes, Algeria.
E-mails: haithem.lazreg@univ-sba.dz and abderrahim.bentaallah@univ-sba.dz.
Corresponding Author: M. H. Lazreg.

The use of a conventional two-level inverter in the field of high power applications is not appropriate because it requires electronic components capable of supporting high reverse voltage and high current [2].

Another disadvantage of this inverter is the problem of magnetic interference caused by the abrupt change of the output voltage of the inverter from zero to high value.

With the appearance of the structures of the multilevel inverters proposed for the first time by [3], the research was able to face the handicaps presented by the classical structure. The aims of this research focus are to improve the quality of the output voltage, as well as to overcome the problems associated with two-level inverters. There are several topologies of multilevel inverters such as floating-diode, floating-capacitor, and cascaded inverters. These structures make it possible to generate an output voltage of several levels.

In high power applications, the structure of the multilevel inverters is the most suitable, compared to the two level structure, because the voltages and output currents have a much lower harmonic distortion rate. The voltage across each switch is halved and the hash frequency is lower.

Diode Clamped Inverter (DCI) is the one that attracts the most attention because of the simplicity of its

structure compared to the floating capacity inverter, in fact, we do not need to use capacities for each phase, which eliminates the risks of parasitic resonances [4]. In this structure, diodes called floating diodes are associated with each phase, which serves to apply the different voltage levels of the DC source.

Modern control techniques lead to control of induction machines comparable to that of the DC machine. Among this techniques, direct torque control, feedback control, vector control, adaptive control.

The Direct Torque Control (DTC) proposed by Takahashi and Depenbrock in 1985 is a solution for the problems of vector control. This technique does not seek the voltages to be applied to the machine, but the best switching state of the inverter to satisfy the user's requirements. It allows us to have a natural decoupling between the flux and the torque, to suppress the PWM stage, to obtain a very good response of the couple [5].
Among the disadvantages of DTCc control that have been shown in the literature include: a slow response for small changes in stator flux and electromagnetic torque, size and complexity of switching tables when the number of levels of inverters is high [6]. In order to improve the performance of the DTCc control, many contributions have been made in the DTC control based on Artificial Neural Networks.

In the field of variable speed drives for machines, the performance of the control laws used depends on the degree of precision in the knowledge of the flux model and its position. Indeed the knowledge of the position of the rotor is indispensable in the control of the double star induction machine. The speed sensor used are fragile, expensive, and affect the reliability of the system [7]. One solution consists in observing or estimating the rotor speed by mathematical algorithms based on information accessible and essential to the control.

In this study, our interest is focused on the extended Kalman filter. It is an observer that provides a good estimate of the state variables of the systems and has shown its effectiveness in different domains [8].

This paper is organized as follows: The DSIM model will be presented in the next section. The five-level inverter modelling is described in the third section. The control method by DTC based on Artificial Neural Networks (DTC-ANN) will be discussed in section four. In the fifth section, we present the theory of the extended Kalman filter. Moreover, in the sixth section the simulation results are discussed on Matlab/Simulink for the proposed control schemes. Finally, a general conclusion summarizes this work.

2 DSIM Model

In the conventional configuration, two identical three-phase windings share the same stator and are shifted by an electric angle of 30°. The rotor structure remains identical to that of a three-phase machine [9].

The model of machine DSIM is nonlinear. With the help of some simplifying assumptions such as:
- the dynamics flux is much slower than that of the stator currents and,
- the dynamics speed is much slower than that of flux.

The DSIM control model fed by voltage static inverter is given by Eqs. (1)-(3) [10]:

$$\frac{dX}{dt} = AX + BU \tag{1}$$

$$T_{em} = p\frac{L_m}{L_r + L_m}\left[\phi_{dr}\left(i_{qs1} + i_{qs2}\right) - \phi_{qr}\left(i_{ds1} + i_{ds2}\right)\right] \tag{2}$$

$$J\frac{d\Omega}{dt} = T_{em} - T_L - k_f\Omega \tag{3}$$

where $X = [x_1, x_2, x_3, x_4, x_5, x_6]^T = [i_{ds1}, i_{ds2}, i_{qs1}, i_{qs2}, \phi_{dr}, \phi_{qr}]^T$, $U = [v_{ds1}, v_{ds2}, v_{qs1}, v_{qs2}]$.

The matrixes A and B are given by:

$$A = \begin{bmatrix} a_1 & a_2 & a_3 & a_4 & a_5 & a_6 \\ -a_2 & a_1 & -a_4 & a_3 & -a_6 & a_5 \\ a_3 & a_4 & a_1 & a_2 & a_5 & a_6 \\ -a_4 & a_3 & -a_2 & a_1 & -a_6 & a_5 \\ a_9 & a_8 & a_7 & 0 & a_7 & 0 \\ -a_8 & a_9 & 0 & a_7 & 0 & a_7 \end{bmatrix},$$

$$B = \begin{bmatrix} b_1 & 0 & b_2 & 0 \\ 0 & b_1 & 0 & b_2 \\ b_2 & 0 & b_1 & 0 \\ 0 & b_2 & 0 & b_1 \end{bmatrix}$$

where $a_1 = b_0\frac{L_m}{T_r} - b_1R_s$, $a_2 = \omega_s\left(b_1L_1 + b_2L_2\right)$,

$a_3 = b_0\frac{L_m}{T_r} - b_2R_s$, $a_4 = \omega_s\left(b_1L_2 + b_2L_1\right)$, $a_5 = \frac{-b_0}{T_r}$,

$a_6 = a_0b_3 + \omega_g b_0$, $a_7 = \frac{L_m}{T_r}$, $a_8 = \omega_g$, $a_9 = -\frac{1}{T_r}$,

$a_{10} = \frac{3}{2}p\frac{L_m}{L_r}$, $\sigma = 1 - \frac{L_m^2}{L_sL_r}$, $L_1 = \sigma L_s$, $L_2 = \sigma L_s - l_s$,

$L_3 = L_s(1-\sigma)$, $a_0 = \frac{L_m}{L_r}$, $b_0 = \frac{L_m}{L_r\left(L_1 + L_2\right)}$,

$b_1 = \frac{L_1}{L_1^2 - L_2^2}$, $b_2 = \frac{L_2}{L_1^2 - L_2^2}$, $b_3 = \omega_s\left(b_1 + b_2\right)$.

3 Modeling of Five-Level Inverter

A five-level three-phase NPC inverter is composed of eight controlled switches that are unidirectional in voltage and bidirectional current, and six holding diodes connected throughout the continuous bus.

The inverter is powered by a continuous source E, which four capacitors of equal values share to give four

separate sources of voltage E/4. The three-phase structure of the NPC inverter with five voltage levels is shown in Fig. 1.

In Fig. 2, there are 60 discrete positions, distributed over four hexes, in addition to a position in the center of the hexagon. Some positions are created by several redundant states. From the outer hexagon to the inner hexagon, the positions of the vector v_s are created respectively by one, two, three or four redundant states. The position of the center of the hexagon, which corresponds to a zero output voltage, is created by five redundant states. There are 24 positions with one redundancy, 18 positions with two redundancies, 12 positions with three redundancies and 6 positions with 04 redundancies. The 61 output voltage vector positions divide the vector diagram into six triangular sectors [11].

For each switch T_{xki} (k = 1, 2, i = 1 ... 8, x = a, b and c), a switching function is defined as follows:

$$F_{xki} = \begin{cases} 1 & \text{if } T_{xki} \text{ is ON} \\ 0 & \text{if } T_{xki} \text{ is OFF} \end{cases} \quad (4)$$

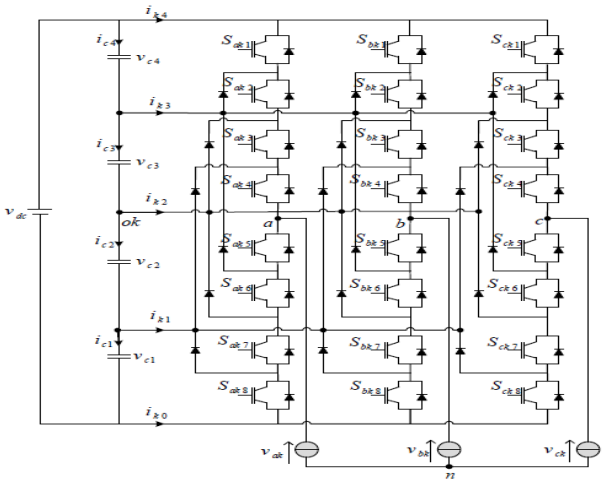

Fig. 1 Diagram of the five level inverter with NPC structure.

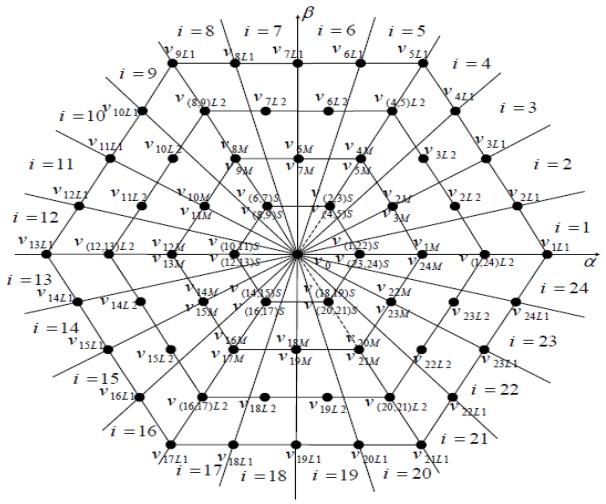

Fig. 2 Vector diagram of the five-level inverter.

The switch control of the lower half-arms are complementary to those of the upper half-arms.

$$F_{xki} = 1 - F_{xk(i-4)} \quad (5)$$

Table 1 summarizes the correspondence between the states of each arm, the states of its switches and its output voltage.

We define five connection functions, each associated with one of the five states of the arm:

$$\begin{cases} F_{c1xk} = F_{c1xk} F_{c2xk} F_{c3xk} F_{c4xk} \\ F_{c2xk} = F_{c2xk} F_{c3xk} F_{c4xk} F_{c5xk} \\ F_{c3xk} = F_{c3xk} F_{c4xk} F_{c5xk} F_{c6xk} \\ F_{c4xk} = F_{c4xk} F_{c5xk} F_{c6xk} F_{c7xk} \\ F_{c5xk} = F_{c5xk} F_{c6xk} F_{c7xk} F_{c8xk} \end{cases} \quad (6)$$

The potentials of the nodes a, b and c of the three-phase inverter at five levels with respect to the point o are given by the following system:

$$\begin{pmatrix} v_{a0k} \\ v_{b0k} \\ v_{c0k} \end{pmatrix} = \begin{pmatrix} F_{c1ak} & F_{c2ak} & F_{c3ak} & F_{c4ak} & F_{c5ak} \\ F_{c1bk} & F_{c2bk} & F_{c3bk} & F_{c4bk} & F_{c5bk} \\ F_{c1ck} & F_{c2ck} & F_{c3ck} & F_{c4ck} & F_{c5ck} \end{pmatrix} \times \begin{pmatrix} v_{c3} + v_{c4} \\ v_{c3} \\ 0 \\ -v_{c2} \\ -(v_{c1} + v_{c2}) \end{pmatrix} \quad (7)$$

4 Direct Torque Control Based on Neural Network

The Direct Torque Control (DTC) of a DSIM is based on the direct determination of the control sequence applied to the switches of a voltage inverter. This choice is based generally on the use of hysteresis comparators whose function is to control the state of the system, namely the amplitude of the stator flux and the electromagnetic torque [12].

In the structure of the DTC, the voltage model is commonly used. Thus, the amplitude of the stator flux is estimated from its components following the axes (α, β).

Table 1 States of an arm of the inverter with five levels.

Switching States	State of the Switches of an Arm								Output Voltage
	T_{xk1}	T_{xk2}	T_{xk3}	T_{xk4}	T_{xk5}	T_{xk6}	T_{xk7}	T_{xk8}	
4	1	1	1	1	0	0	0	0	$v_{c3}+ v_{c4}$
3	0	1	1	1	1	0	0	0	v_{c3}
2	0	0	1	1	1	1	0	0	0
1	0	0	0	1	1	1	1	0	- v_{c2}
0	0	0	0	0	1	1	1	1	-(v_{c1}+v_{c2})

$$\begin{cases} \hat{\varphi}_{\alpha s} = \int_0^t (V_{\alpha s} - R_s I_{\alpha s})\, dt \\ \hat{\varphi}_{\beta s} = \int_0^t (V_{\beta s} - R_s I_{\beta s})\, dt \end{cases} \quad (8)$$

The stator flux module is given by:

$$\hat{\phi}_s = \sqrt{\hat{\phi}_\alpha^2 + \hat{\phi}_\beta^2} \quad (9)$$

The angle θ_s is given by:

$$\hat{\theta}_s = \tan 2^{-1}\left(\frac{\hat{\phi}_\beta(t)}{\hat{\phi}_\alpha(t)}\right) \quad (10)$$

This method of estimating the stator flux has the advantage of simplicity and accuracy, particularly at medium and high speeds where the ohmic voltage drop becomes negligible [13].

The electromagnetic torque can be estimated from the estimated magnitudes of the stator flux, and the measured magnitudes of the line currents, by the equation:

$$\hat{T}_{em} = \frac{3}{2} p.(\hat{\varphi}_{\alpha s} i_{\beta s} - \hat{\varphi}_{\beta s} i_{\alpha s}) \quad (11)$$

This relationship shows that the accuracy of the estimated torque amplitude depends on the accuracy of the stator flux estimator and the current measurement.

Depending on the states of the inverter, the vector v_o can take several positions in the plane α, β. These positions are shown in the vector diagram of Fig. 2.

Table 2 Switching table of the five-level inverter supplying the first star of the DSIM.

φ	τ	Z_i	φ	τ	Z_i	φ	τ	Z_i
	4	V(i+4)L1		4	V(i+6)L1		4	V(i+8)L1
	3	V(i+4)L2		3	V(i+6)L2		3	V(i+8)L2
	2	V(i+4)M		2	V(i+6)M		2	V(i+8)M
	1	V(i+4)S		1	V(i+6)S		1	V(i+8)S
1	0	V0	0	0	V0	-1	0	V0
	-1	V(i+20)S		-1	V(i+18)S		-1	V(i+16)S
	-2	V(i+20)M		-2	V(i+18)M		-2	V(i+16)M
	-3	V(i+20)L2		-3	V(i+18)L2		-3	V(i+16)L2
	-4	V(i+20)L1		-4	V(i+18)L1		-4	V(i+16)L1

Table 3 Switching table of the five-level inverter supplying the second star of the DSIM.

φ	T	Z_i	φ	τ	Z_i	φ	τ	Z_i
	4	V(i+2)L1		4	V(i+4)L1		4	V(i+6)L1
	3	V(i+2)L2		3	V(i+4)L2		3	V(i+6)L2
	2	V(i+2)M		2	V(i+4)M		2	V(i+6)M
	1	V(i+2)S		1	V(i+4)S		1	V(i+6)S
1	0	V0	0	0	V0	-1	0	V0
	-1	V(i+18)S		-1	V(i+16)S		-1	V(i+14)S
	-2	V(i+18)M		-2	V(i+16)M		-2	V(i+14)M
	-3	V(i+18)L2		-3	V(i+16)L2		-3	V(i+14)L2
	-4	V(i+18)L1		-4	V(i+16)L1		-4	V(i+14)L1

Tables 2 and 3 summarize, in general, the active voltage sequences to be applied to increase or decrease the stator flux module and the electromagnetic torque depending on the zone.

4.1 Neural Network Strategy

The human brain is able to adapt, learn and decide, and it is on this fact that researchers have been interested in understanding its operating principle and being able to apply it to the field of computer science.

Among the disadvantages of DTCc control a slow response for small changes in stator flux and electromagnetic torque, size and complexity of switching tables when the number of levels of inverters is high. In order to improve the performance of the DTCc control many contributions have been made in the DTC control based on Artificial Neural Networks (DTC-ANN) [14].

In this application, our goal is to replace switching tables with artificial neural networks.

The multilayer architecture was chosen to be applied to multi-level DTC control. This network, which can be multiplexed for each controller output, has acceptable performance in many industrial applications [15]. The neural network contains three layers: input layer, hidden layers, and output layer. Each layer consists of several neurons. The number of neurons in the output and the layers depends on the number of input and output variables chosen. The number of hidden layers and the number of neurons in each one depend on the dynamics of the system and the desired degree of accuracy.

Fig. 3 shows the structure of the neural network applied to the five-level DTC control of the DSIM. Where the switching tables of the five-level DTC are used as matrix tables. It is a network with three neurons in the input layer, whose inputs are: flow error (E_f), torque error (E_c) and flow position angle (Z). Thus, 24 neurons in the hidden layer, and 12 neurons in the output. Fig. 4 shows the chosen architecture [16].

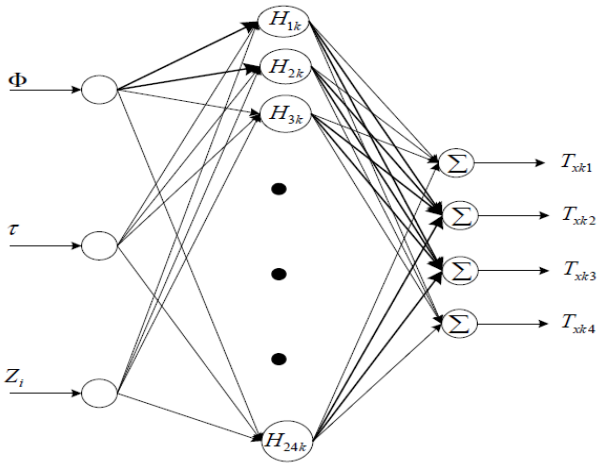

Fig. 3 Neural network structure applied to the five-level DTC control.

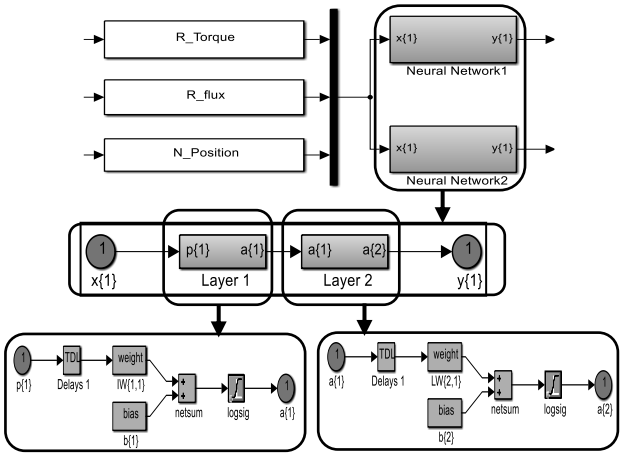

Fig. 4 Selection table based on neuron network.

5 Extended Kalman Filter (EKF)

In the family of observers, the Kalman filter presupposes the presence of noise on the state and on the output. The natural presence of noises, when an asynchronous machine is driven by an inverter, represents an argument for this choice.

The Kalman filter solves, in the time domain, the problem of statistical estimation for linear systems. It uses the state representation of stochastic linear systems. It then provides an optimal estimate in the sense of the minimum variance as well as the variance of the estimation error [17].

In our application, the Kalman filter will be used for the estimation of the state vector x_k composed of stator currents, stator fluxes on the two axes (α, β), the rotor position and the mechanical speed. The electrical parameters of the machine are assumed to be known; a preliminary estimate of these parameters is therefore necessary. Thus, from the discrete representation of the double-star synchronous machine, a state observer is constructed.

This filter is based on a number of assumptions, including noise. Indeed, they assume that the noises that affect the model are centered and white and that they are decorrelated from the estimated states. In addition, state noises must be decorrelated from the measurement noises.

Given the following nonlinear stochastic model:

$$\begin{cases} x(k+1) = f\left(x(k), u(k)\right) + w(k) \\ y(k) = h\left(x(k)\right) + v(k) \end{cases} \tag{12}$$

with

$w(k)$: State noise vector,

$v(k)$: Measurement noise vector.

This nonlinear system is brought back into a linear system and all the equations of the extended Kalman filter are deduced. The estimation procedure is divided into two stages:

First step: Prediction phase

Estimate in the form of a prediction:

$$\hat{x}(k+1/k) = f\left(\hat{x}(k/k), u(k)\right) \tag{13}$$

This step makes it possible to construct a first estimate of the state vector at the instant (k+1). We then try to determine its variance.

Calculation of the covariance matrix of the prediction error:

$$P(k+1/k) = F(k)P(k)F(k)^T + Q \tag{14}$$

with

$$F(k) = \left.\frac{\partial f\left(x(k), u(k)\right)}{\partial x^T(k)}\right|_{x(k)=\hat{x}(k/k)} \tag{15}$$

The prediction phase makes it possible to have a difference between the measured output y_{k+1} and the predicted output $y_{k+1/k}$. To improve the state, it is necessary to take into account this difference and to correct it by means of the gain of the filter K_{k+1}. By minimizing the variance of the error [18], we obtain the following expressions:

Calculation of Kalman gain:

$$K(k+1) = P(k+1/k)H(k)^T \times \left(H(k)P(k+1/k)H(k)^T + R\right)^{-1} \tag{16}$$

with

$$K(k) = \left.\frac{\partial h\left(x(k)\right)}{\partial x(k)}\right|_{x(k)=\hat{x}(k)} \tag{17}$$

Calculation of the covariance matrix of the filter error:

$$P(k+1/k+1) = P(k+1/k) - K(k+1)H(k)P(k+1/k) \tag{18}$$

Estimation of the state vector at (k + 1):

$$\hat{x}(k+1/k+1) = \hat{x}(k+1/k) - K(k+1)\left(y(k+1) - H\hat{x}(k+1/k)\right) \tag{19}$$

Fig. 5 shows the schematic diagram of the extended Kalman filter.

The matrix Q linked to the noises disturbing the state makes it possible to regulate the quality of estimation of our modelling and its discretization. A higher value of Q gives a high value of the gain K reducing the importance of the modelling and the dynamics of the filter. The measurement then has a larger relative weight. A high value of Q can, however, create instability of the observer.

The matrix R regulates the weight of the measurements. A high value indicates a great

uncertainty of the measurement. On the other hand, a low value makes it possible to give a significant weight to the measurement. However, attention must be paid to the risk of instability at low R values.

The extended state vector chosen is: $x(t) = [i_\alpha\ i_\beta\ \varphi_\alpha\ \varphi_\beta\ \Omega\ \theta]$, $y = [i_\alpha\ i_\beta]$, u = $[v_\alpha\ v_\beta]$.

To estimate the speed of rotation of the DSIM by extended Kalman filter, the measurement of the stator currents and the estimation of the voltage vector are essential. The estimate made by adopting the following observer parameters:

$$Q = \begin{bmatrix} 100 & 0 & 0 & 0 & 0 & 0 \\ 0 & 100 & 0 & 0 & 0 & 0 \\ 0 & 0 & 0.1 & 0 & 0 & 0 \\ 0 & 0 & 0 & 0.1 & 0 & 0 \\ 0 & 0 & 0 & 0 & 0.1 & 0 \\ 0 & 0 & 0 & 0 & 0 & 0.1 \end{bmatrix}, \quad R = \begin{bmatrix} 0.12 & 0 \\ 0 & 0.12 \end{bmatrix},$$

$$P = \begin{bmatrix} 0.1 & 0 & 0 & 0 & 0 & 0 \\ 0 & 0.1 & 0 & 0 & 0 & 0 \\ 0 & 0 & 10^{-5} & 0 & 0 & 0 \\ 0 & 0 & 0 & 10^{-5} & 0 & 0 \\ 0 & 0 & 0 & 0 & 10^{-5} & 0 \\ 0 & 0 & 0 & 0 & 0 & 0.1 \end{bmatrix}.$$

Fig. 6 shows the principle of the direct multilevel torque control applied to double star induction machine without a speed sensor using the extended Kalman filter.

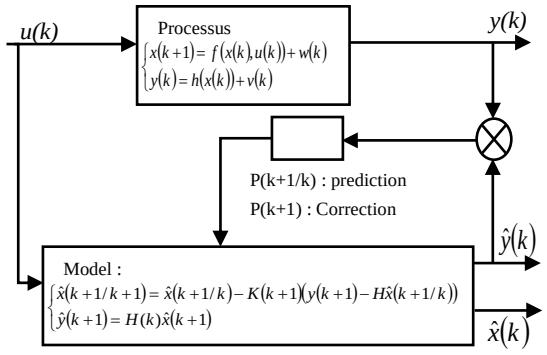

Fig. 5 Principle of the extended Kalman filter.

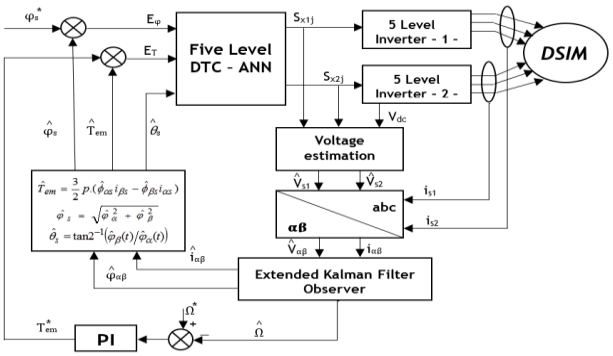

Fig. 6 Five-level DTC-ANN scheme for sensorless DSIM using extended Kalman Filter.

6 Simulation Results

In order to test the static and dynamic performance of the sensorless control, the DSIM is accelerated from standstill to reference speed 100 rad/s. The machine is applied with a load torque of 11Nm. Finally, the direction of rotation of the machine is reversed from 100 rad/s to -100 rad/s at time t = 2s. Figs. 7 and 8 show the simulation results of the five-level DTC control for sensorless DSIM using the extended Kalman filter.

Simulation results of real and estimated speed, stator flux, torque, stator current and stator voltage show the good performance of the five level DTC-ANN control of DSIM (speed, stability and precision).

We note that the speed follows its reference value. The electromagnetic torque stabilizes at the value of the nominal torque after a transient regime with rapid response and without exceeding before stabilizing at the value of the applied load torque. The stator flux is a constant value and it is found that the behaviour of the stator flux and the electromagnetic torque are independent thus confirming a total decoupling.

During rotation sense's reversing, the speed controller shows a similar behaviour as the starting up state by operating the system at the physical limit. The speed and torque response show good dynamic and reference tracking while transient and steady state. The magnitude and the trajectory illustrate that the flux takes a few steps before reaching the reference value 2.2Wb. The stator current show good sinusoid waveform.

Concerning the estimation of the rotor speed, the results of simulation show that the superposition of the estimated and real speeds; the error between the real speed and its estimated value tends to zero.

On the other hand, the five level DTC control significantly reduces the torque and flux ripple, and the THD value of the stator current compared to the five level DTC control.

From these simulation results, it is noted that the output voltage form depends on the number of levels of the inverter used. Regarding the evolution of the harmonic distortion rate (THD) of the output voltage, we note that it equals 3.98%.

6.1 Low Speed Operation

Fig. 9 show the simulation results of the five-level DTC control of sensorless DSIM using the extended Kalman filter for low speed operation. DSIM is accelerated from standstill to a low reference speed of 10 rad/s, at time t = 0.5 s the DSIM is accelerated again to a reference speed of 100 rad/s. The machine is loaded with a nominal load of 11 Nm. Finally, a reversal of the direction of rotation from 100 rad/s to -10 rad/s is performed at time t = 2s.

The simulation results show that low speed operation does not affect the performance of the proposed drive. Indeed the decoupling between the torque and the flux is guaranteed, the good reference speed tracking is

ensured, and the speed estimation is effective.

7 Conclusions

From the results of simulation of the DTC-ANN control of the sensorless DSIM fed by two multilevel inverters, we realize that it is a decoupled control ensuring a good speed continuation, an effective rejection of the disturbance and a good observation of the speed.

The simulation results obtained show that this control technique makes it possible to obtain a perfect decoupling between the stator flux and the electromagnetic torque with fast tracking dynamics. In addition, the estimation of the speed is very satisfactory even at low speed. The introduction of the stabilization strategy in the DTC-ANN control makes it possible to give an added value to the drive system from the point of view of balancing the voltages across the capacitors at the input of the inverter and the reduction of the corrugations of the electromagnetic torque and stator flux.

The simulation results confirm that the proposed multiphase drive has excellent performance at high speeds and estimating rotor speed. However, it is necessary to test its operation at low speeds.

It can be seen that the use of multilevel inverters makes it possible to have a charging current close to a sinusoidal shape while decreasing the ripples of the torque, to obtain a short transient regime and to supply the machine with a voltage of the low THD.

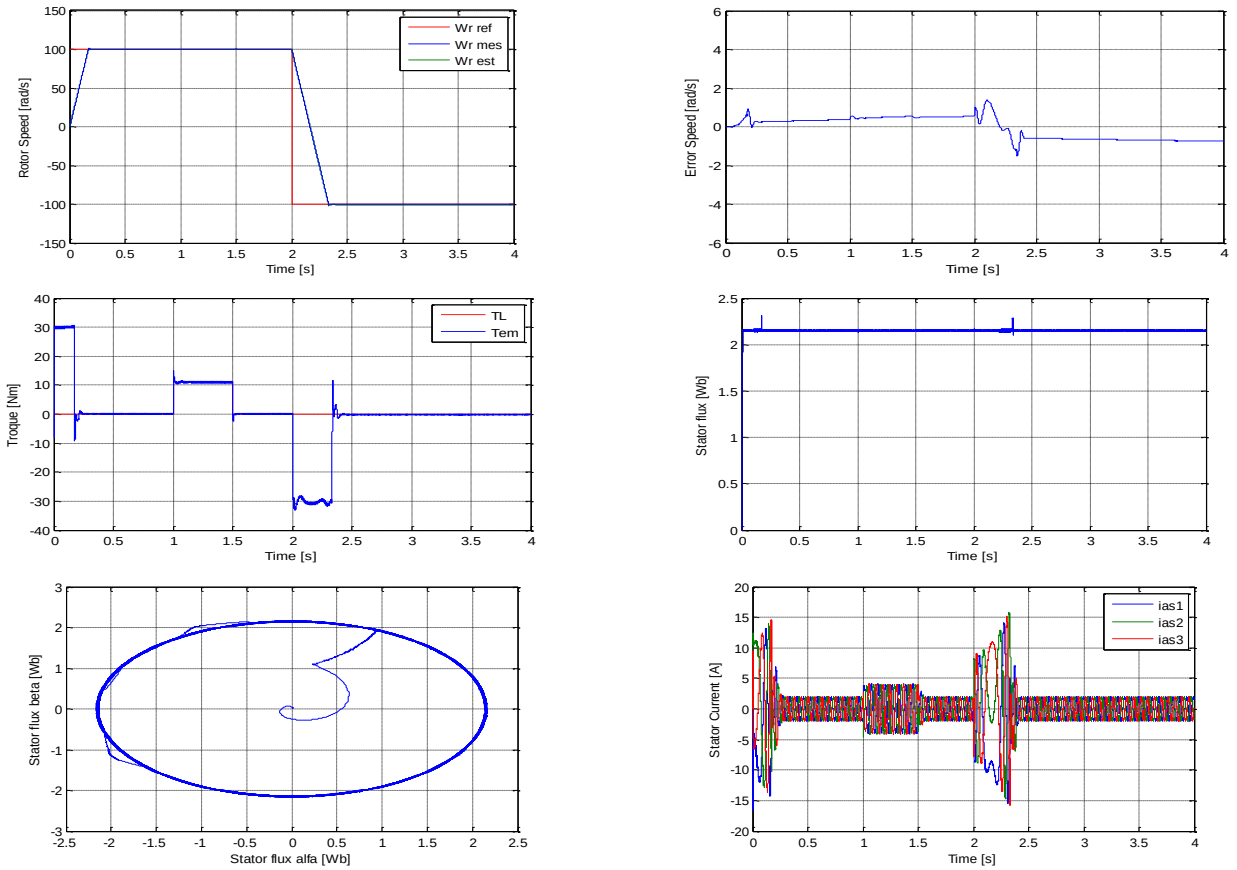

Fig. 7 Simulation results of real and estimated speed, torque, stator flux and current of five level DTC-ANN.

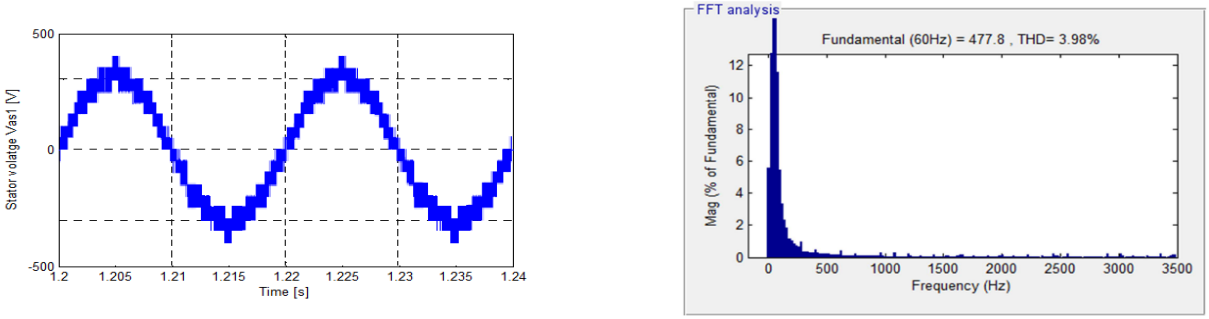

Fig. 8 Simulation results of stator voltage and THD of five level DTC-ANN.

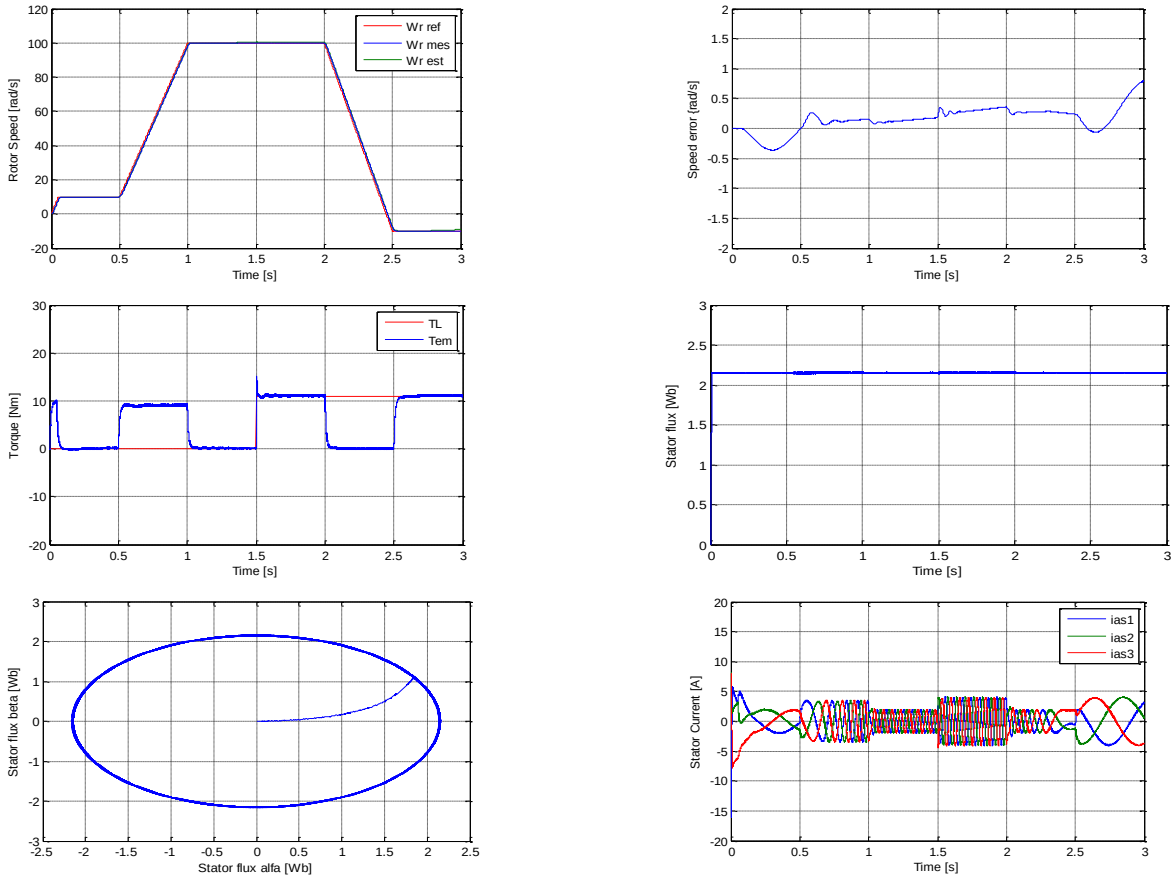

Fig. 9 Simulation results of real and estimated speed, torque, stator flux and current of five level DTC-ANN for low speed operation.

Appendix

DSIM Parameters

P_n = 4.5 Kw, I_n = 6 A, R_r = 2.12 Ω, R_{s1} = R_{s2} = 1.86 Ω, L_{s1} = L_{s2} = 0.011 H, L_m = 0.3672 H, J = 0.065 Kg.m², L_r = 0.006 H.

Acknowledgments

This work was financially supported by the Electrical Engineering Department, Djillali Liabes University, Sidi Bel Abbes of Algeria. The authors would like to thank the members of laboratory Intelligent Control and Electrical power Systems (ICEPS) for their precious suggestions.

References

[1] K. Sahraoui, K. Kouzi, and A. Ameur, "Optimization of MRAS based speed estimation for speed sensorless control of DSIM via genetic algorithm," *Electrotehnica, Electronica, Automatica (EEA)*, Vol. 65, No. 3, pp. 156–162, 2017.

[2] B. Kirankumar, Y. V. Siva Reddy, and M. Vijayakumar, "Multilevel inverter with space vector modulation: intelligence direct torque control of induction motor," *IET Power Electronics*, Vol. 10, No. 10, pp. 1129–1137, 2017.

[3] S. Payami, R. K. Behera, and A. Iqbal, "DTC of three-level NPC inverter fed five-phase induction motor drive with novel neutral point voltage balancing scheme," *IEEE Transactions on Power Electronics*, Vol. 33, No. 2, pp. 1487–1500, 2018.

[4] P. Naganathan and S. Srinivas, "Five-level torque controller-based DTC method for a cascaded three-level inverter fed induction motor drive," *IET Power Electronics*, Vol. 10, No. 10, pp. 1223–1230, 2017.

[5] A. Taheri, "Harmonic reduction of direct torque control of six-phase induction motor," *ISA Transactions*, Vol. 63, pp. 299–314, 2016.

[6] A. Khedher and F. Mimouni, "Sensorless adaptive DTC of double star induction motor," *Energy Conversion and Management*, Vol. 51, pp. 2878–2892, 2010.

[7] M. H. Lazreg and A. Bentaallah, "Speed sensorless vector control of double star induction machine using reduced order observer and MRAS estimator," *IEEE International Conference on Electrical Engineering (ICEE-B)*, Boumerdes, Algeria, 29-31 Oct. 2017.

[8] I. Alsofyani, N. Rumzi, and N. Idris, "Lookup-table-based DTC of induction machines with improved flux regulation and extended Kalman filter state estimator at low-speed operation," *IEEE Transactions on Industrial Informatics*, Vol. 12, No. 4, pp. 1412–1425, 2016.

[9] A. Meroufel, S. Massoum, A. Bentaallah, and P. Wira, "Double star induction motor direct torque control with fuzzy sliding mode speed controller," *Rev. Roum. Sci. Techn– Électrotechn and Énerg*. Vol. 62, No. 1, pp. 31–35, 2017.

[10] A. Khedher and M. F. Mimouni, "Sensorless-adaptive field oriented control of a double star induction machine," in *ecologic vehicles renewable energies*, Monaco, 2009.

[11] A. Rosmadi, A. Nasrudin, R. Siti, and R. Sheikh, "Five-level diode-clamped inverter with three-level boost converter," *IEEE Transactions on Industrial Electronics*, Vol. 61, No. 10, pp. 5155–5163, 2014.

[12] V. Talaeizadeh and R. Kianinezhad, "Direct torque control of six-phase induction motors using three-phase matrix converter," *Energy Conversion and Management*, Vol. 51, No. 12, pp. 2482–2491, 2010.

[13] A. Usta, I. Okumus, and A. Kahveci, "Simplified three-level SVM-DTC induction motor drive with speed and stator resistance estimation based on extended Kalman filter," *Electrical Engineering*, Vol. 99, No. 2, pp. 707–720, 2017.

[14] K. Barika and K. Jaladi, "Five-phase induction motor DTC-SVM scheme with PI controller and ANN controller," *Procedia Technology*, Vol. 25, pp. 816–823, 2016.

[15] M. Zolfaghari, S. A. Taher, and D. V. Munuz, "Neural network-based sensorless direct power control of permanent magnet synchronous motor," *Ain Shams Engineering Journal*, Vol. 7, No. 2, pp. 729–740, 2016.

[16] M. R. Douiri and M. Cherkaoui, "Comparative study of various artificial intelligence approaches applied to direct torque control of induction motor drives," *Frontiers in Energy*, Vol. 7, No. 4, pp. 456–467, 2013.

[17] E. G. Shehata, "Speed sensorless torque control of an IPMSM drive with online stator resistance estimation using reduced order EKF," *International Journal of Electrical Power & Energy Systems*, Vol. 47, pp. 378–386, 2013.

[18] E. Zerdali and M. Barut, "The comparisons of optimized extended kalman filters for speed-sensorless control of induction motors", *IEEE Transactions on Industrial Electronics*, Vol. 64, No. 6, pp. 4340–4351, 2017.

M. H. Lazreg was born in Algeria in 1991. He received Master's degree in Electrical Engineering in 2015 from Djillali Liabes University, Sidi Bel Abbes. He is currently a Ph.D. student at the same University. He is a member of the ICEPS (Intelligent Control Electrical Power System) Laboratory. His research interests are focused on advanced control of ac drives, sensorless control, and intelligent artificial.

A. Bentaallah was born in Algeria in 1965; He received his BS degree in Electrical engineering from Sidi Bel-Abbes University (Algeria) in 1991, the MS degree from the same University in 2005 and the PhD degree from The University of Sidi Bel-Abbes (Algeria) in 2009. He is currently Professor of Electrical Engineering in this University. He is a member of the ICEPS. His research interests are nonlinear control and observers applied in induction motor.